JACS
JOURNAL OF THE AMERICAN CHEMICAL SOCIETY
pubs.acs.org/JACS
Article

Alkylamine-Substituted Perthiocarbamates: Dual Precursors to Hydropersulfide and Carbonyl Sulfide with Cardioprotective Actions

Vinayak S. Khodade, Blaze M. Pharoah, Nazareno Paolocci, and John P. Toscano*

Cite This: J. Am. Chem. Soc. 2020, 142, 4309–4316
Read Online

ABSTRACT: The recent discovery of hydropersulfides (RSSH) in mammalian systems suggests their potential roles in cell signaling. However, the exploration of RSSH biological significance is challenging due to their instability under physiological conditions. Herein, we report the preparation, RSSH-releasing properties, and cytoprotective nature of alkylamine-substituted perthiocarbamates. Triggered by a base-sensitive, self-immolative moiety, these precursors show efficient RSSH release and also demonstrate the ability to generate carbonyl sulfide (COS) in the presence of thiols. Using this dually reactive alkylamine-substituted perthiocarbamate platform, the generation of both RSSH and COS is tunable with respect to half-life, pH, and availability of thiols. Importantly, these precursors exhibit cytoprotective effects against hydrogen peroxide-mediated toxicity in H9c2 cells and cardioprotective effects against myocardial ischemic/reperfusion injury, indicating their potential application as new RSSH- and/or COS-releasing therapeutics.

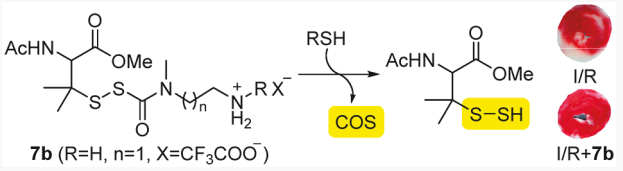

INTRODUCTION

The discovery of H_2S as an endogenously produced signaling molecule has stimulated interest in H_2S-derived species as possible biological mediators. H_2S signaling is proposed to occur via post-translational modification of protein cysteine residues (RSH) to form hydropersulfides (RSSH),[1−4] and recent reports indicate that much of the biological effects attributed to H_2S could instead be due to RSSH and polysulfides.[5−7] Several reports have shown that small-molecule hydropersulfides such as cysteine hydropersulfide (Cys-SSH) and glutathione hydropersulfide (GSSH) are ubiquitous and highly prevalent in mammalian cells, tissue, and plasma.[1,5,8,9] Furthermore, numerous enzymes and proteins have been reported to have RSSH modifications at many cysteine residues.[10−14] Recently, Akaike and co-workers have shown that Cys-SSH is biosynthesized and attached to tRNA by the cysteinyl tRNA synthetases (CARS) and subsequently is translationally incorporated into proteins.[15] The prevalent nature of RSSH in cells suggests that they could have important biological functions.

RSSH display distinct chemistry, and this may be important for their biological utility. For example, RSSH are superior nucleophiles and more potent reductants than their corresponding thiols because of the presence of unshared electron pairs on the sulfur atom adjacent to the nucleophilic sulfur atom.[16−18] RSSH and related species have been proposed to behave as potent antioxidants and redox signaling intermediates.[5,6,8,9,18−22] Recent reports have demonstrated that RSSH are efficient H atom transfer agents toward alkyl, alkoxyl, peroxyl, and thiyl radicals, confirming their promise as potent antioxidants.[23,24] Unlike thiols, RSSH can also undergo transsulfuration reactions because of their electrophilic properties in the neutral state.[18,25] The sulfane sulfur in RSSH can be reversibly transferred to other free thiols such as glutathione (GSH) or cysteine (Cys-SH) to form GSSH or Cys-SSH, respectively. Furthermore, studies have suggested RSSH involvement in the detoxification of environmental electrophiles.[26−28] Yet, despite the increasing evidence of the role of RSSH in redox signaling, the biological functions of RSSH remain elusive. This deficiency is partly due to the instability of RSSH under physiological conditions.

Small-molecule donors of reactive sulfur species are essential tools that can be used to elucidate their biological chemistry. To this end, several RSSH donors have been reported (Figure 1). For example, precursors containing an activated disulfide bond have been developed to rearrange spontaneously at physiological pH thereby producing RSSH.[29] We recently reported a novel class of S-substituted thioisothioureas as efficient RSSH precursors.[30] Wang and co-workers have developed esterase-sensitive RSSH prodrugs and demonstrated their cardioprotective effects.[31] Similarly, Xian and co-workers have reported fluoride/acid-activated RSSH donors.[32] Recently, H_2O_2-triggered self-immolative RSSH donors have been developed that exhibit cytoprotective effects against oxidative stress.[33,34] These findings highlight the therapeutic potential of small-molecule RSSH donors against oxidative stress-related diseases. Although chemical tools for RSSH generation have emerged, no convenient methodology for the

Received: November 11, 2019
Published: February 14, 2020

https://dx.doi.org/10.1021/jacs.9b12180
J. Am. Chem. Soc. 2020, 142, 4309−4316

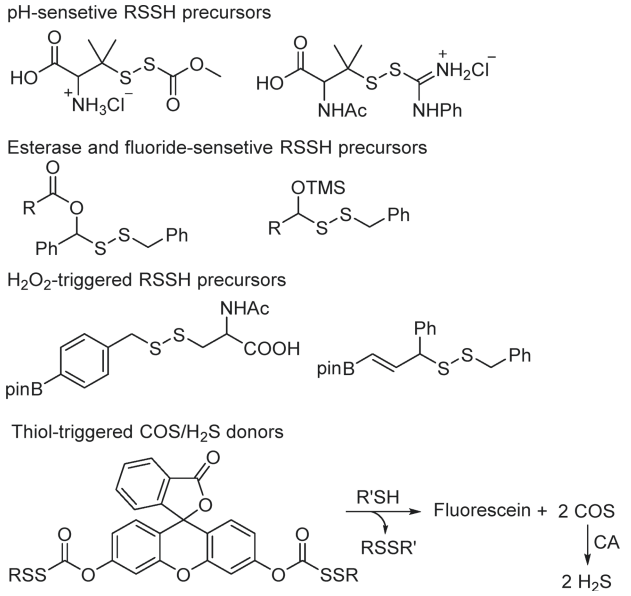

Figure 1. Selected small-molecule RSSH and COS/H_2S donors.

controlled and extended release of RSSH over long time periods is currently available.

Activation of prodrugs via intramolecular cyclization−elimination has been a widely used strategy for drug delivery.[35−37] In this approach, active drug release is dependent upon a predictable intramolecular cyclization−elimination reaction. We envisioned RSSH release using such a strategy with the sulfhydryl group of RSSH protected in the form of perthiocarbamate **1** (Scheme 1) and a terminal non-

Scheme 1. Design of Hydropesulfide/Carbonyl Sulfide Precursors

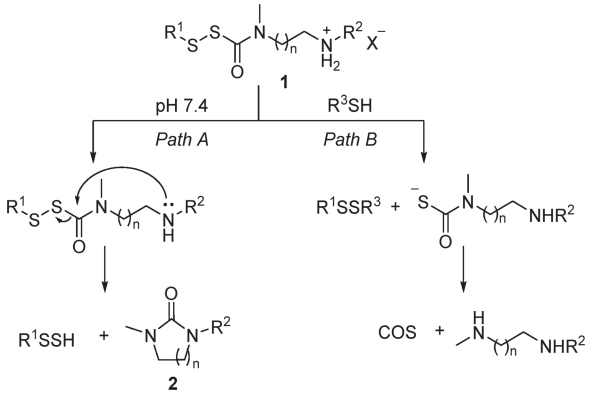

nucleophilic quaternary ammonium salt. As shown in Scheme 1 (Path A), neutralization of the quaternary ammonium salt under physiological conditions forms an active amine nucleophile that can then undergo an intramolecular cyclization to release RSSH and a cyclic urea, presumably a biologically innocuous byproduct. Varying the substituent on the trigger nitrogen and changing the length of the methylene spacer should allow the rate of cyclization to be tuned, thereby varying RSSH release rates. We also reasoned that the alkyl substituent on the perthiocarbamate nitrogen would improve the aqueous stability of these precursors.

Recently, Pluth and co-workers have reported caged sulfenyl thiocarbonates (Figure 1) that release carbonyl sulfide (COS) in the presence of biological thiols.[38] Under physiological condition, COS is rapidly hydrolyzed to H_2S by an ubiquitous enzyme, carbonic anhydrase (CA).[39] The detection of COS in human tissues suggests that it may also have regulatory roles in biology;[40] however, our understanding of these roles remains limited. To advance future investigations into the biological roles of COS, a series of COS donors that are activated by different triggers have been developed.[41−47] We reasoned that perthiocarbamates **1** may also produce COS in the presence of thiols as shown in Scheme 1, Path B. Under biological conditions, the RSSH released from Path A may react further with thiols to produce H_2S. Similarly, COS generated from Path B would be converted to H_2S by CA.

RESULTS AND DISCUSSION

To synthesize alkylamine-substituted perthiocarbamates, *N*-acetyl-cysteine methyl ester was treated with chlorocarbonylsulfenyl chloride to obtain the *S*-perthiocarbonyl chloride **3**, which was immediately reacted with *tert*-butyl methyl(2-(methylamino)ethyl)carbamate in the presence of triethylamine to obtain **4** in 69% overall yield (Scheme 2). The *tert*-butoxycarbonyl (Boc) protecting group was removed by treatment with trifluoroacetic acid to obtain precursor **1a** in 95% yield.

Scheme 2. Synthesis of Hydropesulfide Precursor 1a

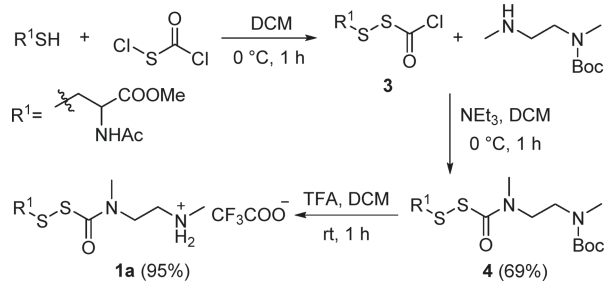

With **1a** in hand, we first examined RSSH generation using ultraperformance liquid chromatography−mass spectrometry (UPLC−MS). We used *β*-(4-hydroxyphenyl)ethyl iodoacetamide (HPE-IAM) as an RSSH trap. HPE-IAM was chosen because it is a soft electrophile and has been widely used to estimate RSSH yields from biological samples.[15,48] Incubation of **1a** with HPE-IAM (50 equiv) in ammonium bicarbonate buffer (pH 7.4, 50 mM) shows RSS-HPE-AM **5** formation (Supporting Information Figure S1; Scheme 3, eq 1), demonstrating the release of RSSH. However, dialkyltrisulfide **6** formation is also observed as a major product (Scheme 3, eq 2), suggesting that precursor **1a** is a competitive trap for the initially released RSSH. As expected, the byproduct 1,3-dimethyl-2-imidazolidinone (**2a**) is observed in 52% yield

Scheme 3. Proposed Mechanism of RSSH and Trisulfide Formation from Precursor 1a

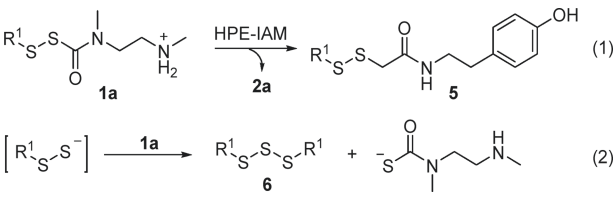

https://dx.doi.org/10.1021/jacs.9b12180
J. Am. Chem. Soc. 2020, 142, 4309−4316

under these conditions, confirming that RSSH release occurs via intramolecular-cyclization reaction. To verify RSSH generation, **1a** was independently incubated with *N*-ethyl maleimide (NEM, 50 equiv) in pH 7.4 buffer, and UPLC–MS analysis shows RSS-NEM adduct formation (Supporting Information Figure S5a). In addition, we observe improved yield of the byproduct **2a** (74%) and decreased level of trisulfide in the presence of NEM (Supporting Information Figure S5b), presumably due to its better RSSH-trapping efficiency vs HPE-IAM.

To minimize the reaction of released RSSH with its precursor, we synthesized donor **7a** (Figure 2), equipped

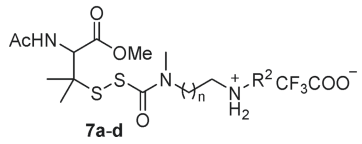

	R^2	n	yield (%)
7a	CH_3	1	96
7b	H	1	97
7c	CH_3	2	94
7d	H	2	96

Figure 2. Structures of RSSH precursors **7a–d** with synthetic yields.

with an inhibiting dimethyl substituent alpha to the disulfide. RSSH generation from **7a** was examined with HPE-IAM trapping and shows RSS-HPE-AM **9** formation with no evidence of dialkyltrisulfide generation (Supporting Information Figure S10).

To support the proposed mechanism for RSSH release, we examined RSSH release from a control compound **8** (Scheme 4) lacking the terminal amine group. No RSSH release is

Scheme 4. Reaction of 8 with *n*-BuNH$_2$ and *N*-Acetyl Cysteine

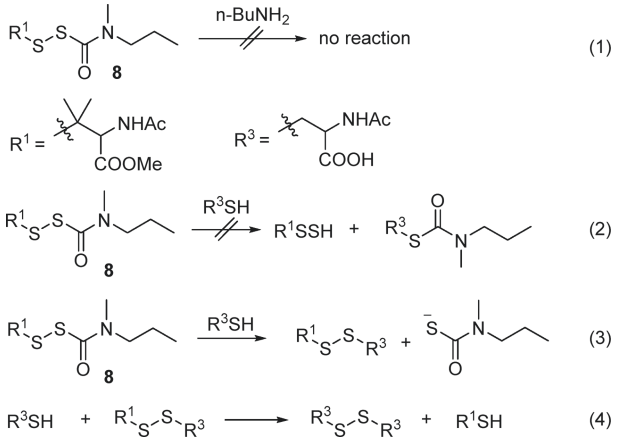

observed from **8** under similar conditions (Supporting Information Figure S25), confirming that the terminal amine is required for precursor activation. We also tested the ability of **8** to release RSSH via intermolecular reactions with amines (Scheme 4, eq 1). However, incubation of **8** with a model amine, *n*-butylamine (5 equiv), shows no reactivity, at least over 2 h (Supporting Information Figure S27), suggesting that **8** is stable under these conditions and does not release RSSH via intermolecular reaction. Additionally, we tested RSSH release from **8** in the presence of *N*-acetyl cysteine (NAC) in pH 7.4 ammonium bicarbonate buffer. We anticipated that if thiol attacks the perthiocarbamate carbonyl group of **8**, we should observe RSSH and/or RSSH-derived polysulfides and the NAC-thiocarbamate byproduct (Scheme 4, eq 2). However, UPLC–MS analysis shows no evidence of these products (Supporting Information Figure S29). Instead, mixed disulfide (R^1SSR^3) formation is observed, presumably formed by the thiol attack on the internal sulfur of compound **8** (Scheme 4, eq 3). Furthermore, mixed disulfide R^1SSR^3 undergoes disulfide exchange reaction with NAC to produce *N*-acetyl cystine (R^3SSR^3) and *N*-acetyl-penicillamine methyl ester (R^1SH) (Scheme 4, eq 4). Together, these results indicate that the control compound **8** does not release RSSH via intermolecular reactions in the presence of amines or thiols.

Next, we monitored the kinetics of RSSH release from **7a** by HPE-IAM trapping in pH 7.4 phosphate buffer at 37 °C using HPLC. An increase in peak intensity at 14.1 min attributed to RSS-HPE-AM **9** is observed (Figure 3b). To quantify RSSH,

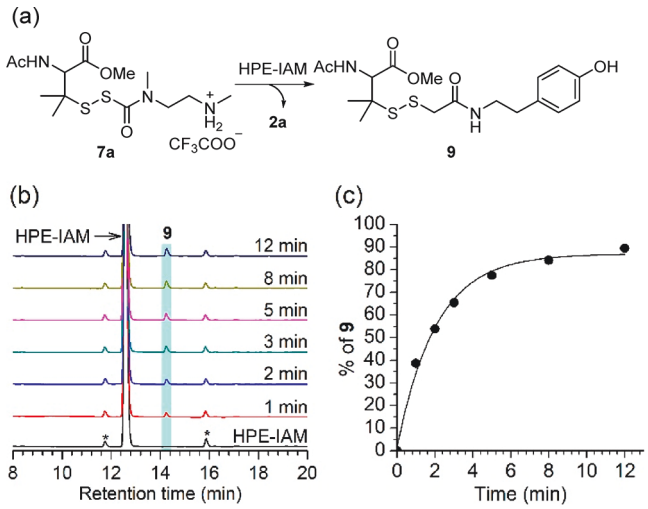

Figure 3. (a) Reaction scheme showing RSSH generation from **7a** in the presence of HPE-IAM. (b) HPLC analysis of RSSH generation from **7a** (100 μM) in the presence of HPE-IAM (5 mM) incubated in pH 7.4 phosphate buffer (100 mM) with DTPA (100 μM) at 37 °C. An aliquot of the reaction mixture was withdrawn at the specified time and quenched with 1% formic acid. Asterisks indicate the presence of impurities in the commercial HPE-IAM sample. (c) Kinetics of RSS-HPE-AM **9** generation. Data represent the average ± SD (n = 3). The curve is the calculated best fit to a single-exponential function (k = 0.505 ± 0.019 min^{-1}; $t_{1/2}$ = 1.4 ± 0.1 min).

we independently synthesized **9** (Supporting Information Scheme S2). HPLC analysis shows 89% formation of **9** from **7a** with a first-order rate constant of k = 0.505 min^{-1} ($t_{1/2}$ = 1.4 min, Table 1). In addition, 87% of byproduct **2a** formation, analyzed using UPLC–MS, is also observed (Supporting Information Figure S10). We also analogously measured the kinetics of **9** (k = 0.58 ± 0.02 min^{-1}; $t_{1/2}$ = 1.2 min) and **2a** (0.57 ± 0.02 min^{-1}; $t_{1/2}$ = 1.2 min) formation from **7a** using

Table 1. Hydropersulfide Yields and Half-Lives for Precursors 7a–d

precursor	R^2	n	hydropersulfide yield (%)[a]	$t_{1/2}$ (min)
7a	CH_3	1	89 ± 3	1.4 ± 0.1
7b	H	1	94 ± 1	16.7 ± 0.3
7c	CH_3	2	90 ± 1	118 ± 4
7d	H	2	82 ± 1	484 ± 10

[a]RSSH precursors (100 μM) were incubated in the presence of HPE-IAM (5 mM) in pH 7.4 phosphate buffer containing DTPA at 37 °C. Reported data represent averages ± SD (n = 3).

https://dx.doi.org/10.1021/jacs.9b12180
J. Am. Chem. Soc. 2020, 142, 4309–4316

UPLC−MS and observed similar rate constants, indicating that RSSH trapping with HPE-IAM is rapid under these conditions (Supporting Information Figure S42). We also examined the effect of pH on the kinetics of RSSH release. As expected, the rate of RSSH release from **7a** decreases at pH 6.0 (k = 0.031 min^{-1}; $t_{1/2}$ = 22.2 min) and increases at pH 8.0 (k = 2.58 min^{-1}; $t_{1/2}$ = 0.27 min).

To tune the kinetics of RSSH release, precursor **7b** with a terminal free amine was synthesized. HPLC analysis shows an increase in half-life (16.7 min, Table 1) at pH 7.4. Similar to that for precursor **7a**, we also observed a pH effect on RSSH release for **7b** ($t_{1/2}$ = 280 min at pH 6.0; $t_{1/2}$ = 5.1 min at pH 8.0). Precursor **7c**, equipped with three methylene spacers, was synthesized to measure its effect on RSSH release. We anticipated that inclusion of a longer spacer compared with that in precursor **7a** would reduce the rate of the intramolecular-cyclization reaction and therefore RSSH release. As expected, the half-life of **7c** increases to 118 min, still with 90% RSSH release. In addition, 88% of the expected byproduct 1,3-dimethyltetrahydropyrimidin-2(1*H*)-one (**2c**) is also observed (Supporting Information Figure S16). Analogously, we also observe significantly slower RSSH release ($t_{1/2}$ = 484 min) from **7d**, equipped with both a terminal free amine and three methylene spacers. Taken together, these results demonstrate the ability of the perthiocarbamate platform to release RSSH efficiently with tunable rates and over long time frames.

The ability of these precursors to release RSSH was also examined in the presence of thiols, likely to be present in significant concentrations under physiological conditions. Because thiols can also readily react with HPE-IAM, we measured RSSH release in its absence. We anticipated that if thiol reaction with the precursor (Scheme 5, eq 2) competes with RSSH release (Scheme 5, eq 1), we should observe reduced yields of RSSH and cyclic ureas **2a−d** and increased formation of thiocarbamate-derived COS and unsymmetrical disulfide **10** (R^1SSR^3). Since RSSH is an unstable species under aqueous conditions, the cyclic-urea yields were measured as an indication of RSSH yield.

When **7a** is incubated with NAC in pH 7.4 buffer, a new peak at 5.67 min with m/z = 238.0556 $[M + H]^+$ corresponding to RSSH (expected m/z = 238.0566) is observed (Figure 4 and Supporting Information Figure S48).

Scheme 5. RSSH and COS Generation from 7a−d in the Presence of Thiol

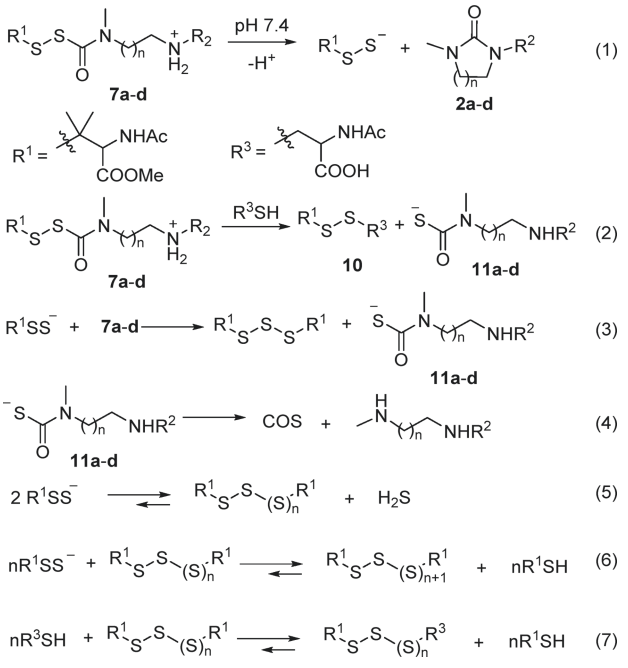

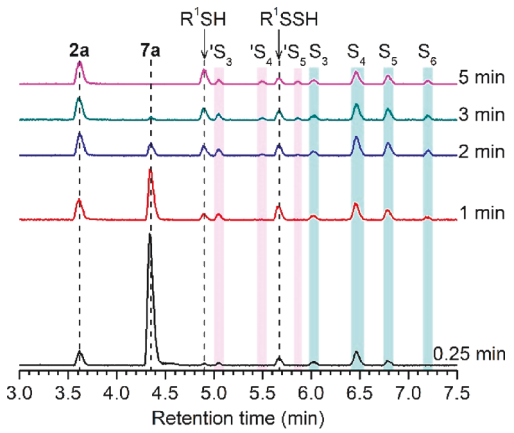

Figure 4. UPLC−MS chromatograms of RSSH generation from **7a** (100 μM) in the presence of NAC (500 μM) incubated in pH 7.4 ammonium bicarbonate (50 mM) with the metal chelator DTPA (100 μM) at 37 °C. Aliquots taken at various times were quenched with 1% formic acid and analyzed by UPLC−MS. A peak at 5.67 min attributed to RSSH is observed under these conditions. RSSH-derived symmetrical dialkyl polysulfide, labeled as S_3−S_6 ($R^1SS_nSR^1$, n = 1−4, cyan highlight), and unsymmetrical dialkyl polysulfides labeled as $'S_3$−$'S_5$ ($R^1SS_nSR^3$, n = 1−3, pink highlight) formation is evident. A peak at 3.62 min attributed to the byproduct **2a** is also observed.

Furthermore, we also observe symmetrical dialkyl polysulfide ($R^1SS_nSR^1$, n = 1−4) formation (Figure 4, cyan highlight), presumably formed by the decomposition of RSSH through disproportionation (Scheme 5, eq 5) and RSSH−polysulfide exchange reactions (Scheme 5, eq 6). In addition, unsymmetrical dialkyl polysulfide ($R^1SS_nSR^3$, n = 1−3) (Figure 4, pink highlight), likely produced by the NAC reaction with symmetrical dialkyl polysulfides, are also observed. The presence of an observable MS peak for RSSH under these conditions is likely due to its equilibrium with polysulfides and its relative stability as a sterically hindered persulfide. Notably, 87% of byproduct **2a** is observed under these conditions (Table 2), suggesting that the efficiency of RSSH generation for short-lived precursor **7a** is unaffected by thiol.

Table 2. Yields of 2a−d from Precursors 7a−d in the Presence of *N*-Acetyl Cysteine

precursor	7a	7b	7c	7d
byproduct %[a]	87 ± 1	58 ± 0.7	19.2 ± 0.5	5.9 ± 0.4

[a]RSSH precursors (100 μM) were incubated in the presence of NAC (500 μM) in pH 7.4 ammonium bicarbonate buffer containing DTPA (100 μM) at 37 °C. Reported data represent averages ± SD (n = 3).

We also examined RSSH generation from **7a** in the absence of a trapping agent. As shown in Supporting Information Figure S54, we again observe a peak at 5.67 min corresponding to RSSH as well as polysulfides ($R^1SS_nSR^1$, n = 1−4) and *N*-acetyl-penicillamine methyl ester, indicating that RSSH undergoes disproportionation reactions and its presence is

https://dx.doi.org/10.1021/jacs.9b12180
J. Am. Chem. Soc. 2020, 142, 4309−4316

likely due to equilibrium reactions with polysulfides. In contrast, UPLC−MS analysis of RSSH release from precursor **1a** in the absence of trap shows no evidence of an MS-observable RSSH peak (Supporting Information Figure S62), consistent with the relatively unstable nature of primary alkyl persulfides.

We also examined thiocarbamate **11a** formation, another anticipated product of precursor **7a** reaction with NAC (Scheme 5, eq 2). UPLC−MS analysis showed no evidence of thiocarbamate formation, suggesting that if formed, it rapidly decomposes under aqueous conditions to release COS (Scheme 5, eq 4). We monitored COS production using membrane inlet mass spectrometry (MIMS), a technique used to detect hydrophobic gases dissolved in aqueous solution using semipermeable membrane that allows gases and not the liquid phase to enter a mass spectrometer.[49] When precursor **7a** is examined in the absence of NAC, a very small increase in the m/z = 60 signal attributed to COS (Figure 5a) is observed,

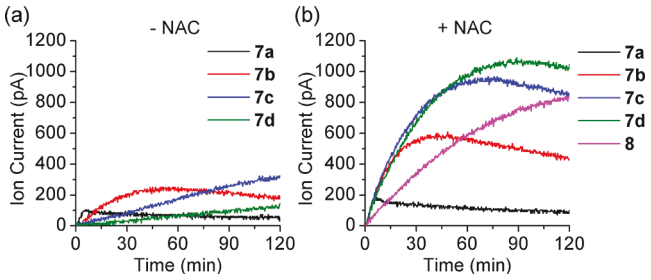

Figure 5. COS measurement using MIMS generated from **7a−d** (50 μM) either (a) without NAC or (b) with NAC (0.25 mM, 5 equiv) in pH 7.4 phosphate buffer saline (10 mM) with DTPA (100 μM) at 37 °C.

likely arising from released RSSH reaction with precursor **7a** producing thiocarbamate **11a**, which subsequently decomposes to give COS (Scheme 5, eqs 3 and 4). Only a small additional increase in COS signal (Figure 5b) is observed in the presence of NAC, suggesting that **7a** rapidly releases RSSH (Scheme 5, eq 1) and thus is less available to react with NAC (Scheme 5, eq 2). Taken together, these results again demonstrate that **7a** mainly produces RSSH, even in the presence of thiols.

Next, precursor **7b** decomposition was examined in the presence of NAC. UPLC−MS analysis shows decreased byproduct **2b** yield (58%) and reduced levels of $R^1SS_nSR^1$ and $R^1SS_nSR^3$ (Suporting Information Figure S70). Consistent with this observation, we also observe increased production of COS (Figure 5b). These results suggest that with decreasing RSSH release rate, precursor reaction with thiol becomes more competitive. Furthermore, we observe mainly unsymmetrical disulfide **10** (Suporting Information Figures S84 and S90) and COS (Figure 5b) and reduced yields of **2c** and **2d** (Table 2) from precursors **7c** and **7d**, respectively, in the presence of NAC. These results indicate that donors **7c** and **7d** produce mainly COS in the presence of thiol. In addition to COS formation, thiocarbamates **11b−d** can also potentially undergo an intramolecular cyclization to produce cyclic ureas **2b−d** and H_2S. However, we observe reduced yields of **2b−d** during **7b−d** decomposition in the presence of NAC, indicating that this cyclization reaction is not a major contributor. Furthermore, the predicted pK_a of the thiocarbamate sulfhydryl group is ca. 5.5,[50] indicating that it will be predominantly present in anionic form at pH 7.4, thus disfavoring intramolecular cyclization to release H_2S.

We also examined the control compound **8** for COS release under similar conditions. Relatively slow COS release compared with that from **7a−d** is found (Figure 5b). This result suggests that in the cases of precursors **7a−d**, in addition to the thiol-mediated COS release pathway (Scheme 5, eq 2), RSSH reaction with the precursor to produce the thiocarbamate intermediate (Scheme 5, eq 3) presumably contributes to the observed enhanced rate of COS release.

Although partial COS production is observed from longer-lived precursors **7b−7d** in the presence of thiols, the COS generation pathway might be disfavored under certain conditions. For example, patients with cardiovascular disease often have reduced levels of glutathione.[51,52] This result implies that under reduced thiol levels, these precursors may favor the RSSH generation pathway. Furthermore, during myocardial ischemia injury, the local pH changes to mildly acidic,[53,54] and under these conditions, thiol reaction with the RSSH precursor may be diminished. Based on these conditions, we examined COS release from **7b−d** with NAC in pH 6.0 buffer at 37 °C. As expected, we observe diminished levels of COS (Supporting Information Figure S106). Under the same conditions, we still observe RSSH release from **7b**, albeit at a slower rate (Figure S96).

We also compared the reactivity of NAC vs GSH with precursor **7b** at pH 7.4. We anticipate that if GSH reaction with the precursor is slower than NAC, we should observe increased yield of RSSH and cyclic urea **2b** (Scheme 5, eq 1) and reduced levels of thiocarbamate-derived COS and unsymmetrical disulfide **10** (R^1SSR^3) (Scheme 5, eq 2). When **7b** is incubated with NAC, UPLC−MS analysis shows 58% of byproduct **2b** formation. In the presence of GSH, we observe a small decrease in **2b** yield (42%), suggesting that GSH reaction with **7b** is slightly faster than NAC. Consistent with this observation, we also observe increased levels of unsymmetrical disulfide (R^1SSR^3) and reduced levels of RSSH-derived symmetrical dialkyl polysulfides ($R^1SS_nSR^1$, n = 1 and 2) and unsymmetrical dialkyl polysulfides ($R^1SS_nSR^3$, n = 1 and 2) (Suporting Information Figure S97) in the case of GSH reaction with **7b**. Additionally, we observe slightly higher/faster COS release from **7b** in the presence of GSH compared with NAC, analyzed by MIMS (Suporting Information Figure 107). Together, these results indicate that precursor **7b** reaction with GSH (pK_a 8.83) is slightly faster than with NAC (pK_a 9.52), likely due to the higher concentration of the corresponding thiolate at neutral pH.[46,55]

Several studies have speculated that intracellular RSSH and related species protect cells from oxidative stress.[5,6,8,9,18−20,23] We sought to determine whether our alkylamine-substituted perthiocarbamates exert protective effects against oxidative stress and myocardial ischemia-reperfusion (I/R) injury. The medium-lived precursor **7b** ($t_{1/2}$ = 16.7 min) was chosen for the studies. First, we measured the cytotoxicity of **7b** on H9c2 myoblasts using the nucleic acid stain, Sytox, a probe for compromised cell membrane integrity.[56] Both precursor **7b** and its byproduct **2b** show no toxicity toward H9c2 cells after 24 h of exposure at varied concentrations (0−150 μM) (Supporting Information Figure S110). We then measured the cytoprotective effects of **7b** against oxidative stress in H9c2 cells. H_2O_2 (200 μM) was given as a pro-oxidant source, and drastically reduced cell viability was observed using CCK-8 staining (Figure 6a).[57,58] However, pretreating myoblasts with

https://dx.doi.org/10.1021/jacs.9b12180
J. Am. Chem. Soc. 2020, 142, 4309−4316

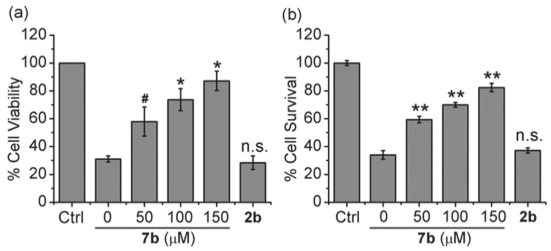

Figure 6. Results from H9c2 cardiac myoblasts pretreated with the RSSH precursor **7b** at (50, 100, and 150 μM) and the byproduct 1-methylimidazolidin-2-one (**2b**) at 150 μM for 2 h followed by exposure to H_2O_2 (200 μM) for 2 h. (a) Quantification of viability was carried out using Cell Counting Kit-8 (CCK-8). Results are expressed as the mean ± SEM (n = 5 for each treatment group) with three independent experiments. (b) Quantification of cytotoxicity was carried out using Sytox Green nucleic acid stain. Results are expressed as the mean ± SEM (n = 5 for each treatment group) with five independent experiments. # $P < 0.05$, * $P < 0.01$, ** $P < 0.001$ for comparisons with the H_2O_2 treatment group. Group comparisons are determined by a one-way analysis of variance (ANOVA) with Dunnett's correction posthoc test using GraphPad Prism 8.

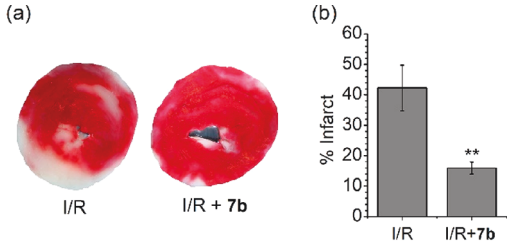

Figure 7. Cardioprotective effects of **7b** postconditioning in the isolated-perfused murine heart. (a) Representative images of coronal slices of the heart following TTC staining. (b) Comparison of the volume of infarcted tissue following ischemia-reperfusion and when the heart is conditioned with precursor **7b** (100 μM) at the onset of reperfusion. Results are expressed as the mean ± SEM (n = 4 for each treatment group) with four independent experiments. ** $P < 0.001$ for comparisons with the IR group. Group comparisons are determined by a one-way analysis of variance (ANOVA) with Dunnett's correction posthoc test using GraphPad Prism 8.

precursor **7b** for 2 h resulted in a dose-dependent attenuation of H_2O_2-induced toxicity (Figure 6a). Under similar conditions, the byproduct **2a** shows no protective effect against H_2O_2-mediated toxicity, suggesting that the protection is due to RSSH and/or COS. Next, the cytoprotective effect of **7b** was independently evaluated using the Sytox assay, due to the potential background reduction of CCK-8 by reactive sulfur species leading to artifactual viability measurements.[26,27] As shown in Figure 6b, **7b** consistently shows protective effects against H_2O_2-mediated toxicity. Under similar conditions, the COS precursor **8** also shows protective effects against H_2O_2-mediated toxicity, but to a lesser extent compared with **7b** (Supporting Information Figure S111). Altogether these results suggest that **7b** is not cytotoxic to cardiac-derived tissue, can be taken up by the cells, and confers protection against oxidative stress.

To build on our results from these in vitro studies, we also tested **7b** in isolated-perfused (ex vivo) mouse hearts. The Langendorff model of myocardial ischemia-reperfusion is a widely used technique whereby the ionotropic and chronotropic effects of a drug can be studied directly without confounding neural/hormonal influences and minimizes changes in coronary vascular tone.[59,60] Following 20 min of global ischemia, **7b** was infused for the first 7 min of reperfusion at a concentration of 100 μM. Reperfusion is continued for a total duration of 90 min before the heart is infused with triphenyltetrazolium chloride (TTC), a stain for determining cellular viability within a given tissue.[61] Figure 7a shows coronal sections of murine hearts stained with TTC. After 20 min global ischemia (I/R), Krebs–Henseleit (KH) perfused hearts show 42% infarct size (Figure 7b). This loss in viable myocardial tissue was significantly attenuated in **7b**-perfused infarcted hearts (16% infarct size). These data demonstrate that RSSH and/or COS can provide protection when given at reperfusion in hearts subjected to I/R injury. Although more work remains to be done to determine the mechanism by which RSSH conditions the tissue to deal with the stress of reperfusion and/or compensates for the damage incurred during ischemia, these data combined with in vitro cellular studies imply that the alkylamine-substituted perthiocarbamates reported here can reduce the extent of myocardial ischemia-reperfusion injury and may be pharmacologically useful.

CONCLUSIONS

In summary, we have prepared alkylamine-substituted perthiocarbamates as a new, versatile, and readily modifiable platform for controllable RSSH release. These precursors show efficient RSSH release with half-lives ranging from 1.4 to 484 min in the presence of HPE-IAM. For long-lived precursors, COS is also produced along with RSSH in the presence of thiols. Alkylamine-substituted perthiocarbamates are an example of prodrugs in which RSSH generation is not dependent upon exogenous reactivity but rather from an intramolecular cyclization–elimination reaction. Furthermore, the terminal amine of these precursors can be conjugated with functional groups that respond to specific stimuli such as light, redox reactions, or enzymes to achieve spatiotemporal control over RSSH release. The potential therapeutic benefit of these precursors has been demonstrated in the context of oxidative stress and myocardial ischemia-reperfusion injury. As such, we anticipate that these precursors will find significant utility as chemical tools for investigating RSSH and COS biology.

ASSOCIATED CONTENT

Supporting Information

The Supporting Information is available free of charge at https://pubs.acs.org/doi/10.1021/jacs.9b12180.

Synthetic procedures, kinetics of RSSH release, analysis of RSSH and COS generation in the presence of thiol, cytotoxicity, cytoprotective, and cardioprotective effects of RSSH/COS precursors, and detailed HRMS, ^{1}H, and ^{13}C NMR data (PDF)

AUTHOR INFORMATION

Corresponding Author

John P. Toscano – *Department of Chemistry, Johns Hopkins University, Baltimore, Maryland 21218, United States;* orcid.org/0000-0002-4277-3533; Email: jtoscano@jhu.edu

Authors

Vinayak S. Khodade – *Department of Chemistry, Johns Hopkins University, Baltimore, Maryland 21218, United States*

https://dx.doi.org/10.1021/jacs.9b12180
J. Am. Chem. Soc. 2020, 142, 4309–4316

Blaze M. Pharoah − *Department of Chemistry, Johns Hopkins University, Baltimore, Maryland 21218, United States*
Nazareno Paolocci − *Division of Cardiology, Johns Hopkins University School of Medicine, Baltimore, Maryland 21205, United States; Department of Biomedical Sciences, University of Padova, Padova, Italy*

Complete contact information is available at: https://pubs.acs.org/10.1021/jacs.9b12180

Notes

The authors declare no competing financial interest.

■ ACKNOWLEDGMENTS

We gratefully acknowledge the National Science Foundation (CHE-1900285 to J.P.T.), the National Institutes of Health (T32 GM080189 for support of B.M.P.; R01 HL136918 and R01 HL063030 to N.P.), and Johns Hopkins University (Magic-That-Matters Fund to N.P.) for generous support for this research. We also thank Dr. Stephen Chelko (Johns Hopkins University) for providing access to a cell culture facility and Drs. Jon Fukuto and Joseph Lin (Sonoma State University) for advice on the cell viability studies.

■ REFERENCES

(1) Mustafa, A. K.; Gadalla, M. M.; Sen, N.; Kim, S.; Mu, W.; Gazi, S. K.; Barrow, R. K.; Yang, G.; Wang, R.; Snyder, S. H. H_2S Signals Through Protein S-Sulfhydration. *Sci. Signaling* **2009**, *2*, ra72−ra72.
(2) Gadalla, M. M.; Snyder, S. H. Hydrogen sulfide as a gasotransmitter. *J. Neurochem.* **2010**, *113*, 14−26.
(3) Filipovic, M. R.; Zivanovic, J.; Alvarez, B.; Banerjee, R. Chemical Biology of H_2S Signaling through Persulfidation. *Chem. Rev.* **2018**, *118*, 1253−1337.
(4) Ju, Y.; Fu, M.; Stokes, E.; Wu, L.; Yang, G. H2S-Mediated Protein S-Sulfhydration: A Prediction for Its Formation and Regulation. *Molecules* **2017**, *22*, 1334.
(5) Ida, T.; Sawa, T.; Ihara, H.; Tsuchiya, Y.; Watanabe, Y.; Kumagai, Y.; Suematsu, M.; Motohashi, H.; Fujii, S.; Matsunaga, T.; Yamamoto, M.; Ono, K.; Devarie-Baez, N. O.; Xian, M.; Fukuto, J. M.; Akaike, T. Reactive cysteine persulfides and S-polythiolation regulate oxidative stress and redox signaling. *Proc. Natl. Acad. Sci. U. S. A.* **2014**, *111*, 7606−7611.
(6) Ono, K.; Akaike, T.; Sawa, T.; Kumagai, Y.; Wink, D. A.; Tantillo, D. J.; Hobbs, A. J.; Nagy, P.; Xian, M.; Lin, J.; Fukuto, J. M. Redox chemistry and chemical biology of H_2S, hydropersulfides, and derived species: Implications of their possible biological activity and utility. *Free Radical Biol. Med.* **2014**, *77*, 82−94.
(7) Toohey, J. I. Persulfide sulfur is a growth factor for cells defective in sulfur metabolism. *Biochem. Cell Biol.* **1986**, *64*, 758−765.
(8) Numakura, T.; Sugiura, H.; Akaike, T.; Ida, T.; Fujii, S.; Koarai, A.; Yamada, M.; Onodera, K.; Hashimoto, Y.; Tanaka, R.; Sato, K.; Shishikura, Y.; Hirano, T.; Yanagisawa, S.; Fujino, N.; Okazaki, T.; Tamada, T.; Hoshikawa, Y.; Okada, Y.; Ichinose, M. Production of reactive persulfide species in chronic obstructive pulmonary disease. *Thorax* **2017**, *72*, 1074−1083.
(9) Kunikata, H.; Ida, T.; Sato, K.; Aizawa, N.; Sawa, T.; Tawarayama, H.; Murayama, N.; Fujii, S.; Akaike, T.; Nakazawa, T. Metabolomic profiling of reactive persulfides and polysulfides in the aqueous and vitreous humors. *Sci. Rep.* **2017**, *7*, 41984.
(10) Massey, V.; Edmondson, D. On the Mechanism of Inactivation of Xanthine Oxidase by Cyanide. *J. Biol. Chem.* **1970**, *245*, 6595−6598.
(11) Branzoli, U.; Massey, V. Evidence for an Active Site Persulfide Residue in Rabbit Liver Aldehyde Oxidase. *J. Biol. Chem.* **1974**, *249*, 4346−4349.
(12) Dóka, É.; Pader, I.; Bíró, A.; Johansson, K.; Cheng, Q.; Ballagó, K.; Prigge, J. R.; Pastor-Flores, D.; Dick, T. P.; Schmidt, E. E.; Arnér, E. S. J.; Nagy, P. A novel persulfide detection method reveals protein persulfide- and polysulfide-reducing functions of thioredoxin and glutathione systems. *Sci. Adv.* **2016**, *2*, No. e1500968.
(13) Longen, S.; Richter, F.; Köhler, Y.; Wittig, I.; Beck, K.-F.; Pfeilschifter, J. Quantitative Persulfide Site Identification (qPerS-SID) Reveals Protein Targets of H2S Releasing Donors in Mammalian Cells. *Sci. Rep.* **2016**, *6*, 29808.
(14) Wright, C. M.; Christman, G. D.; Snellinger, A. M.; Johnston, M. V.; Mueller, E. G. Direct evidence for enzyme persulfide and disulfide intermediates during 4-thiouridine biosynthesis. *Chem. Commun.* **2006**, 3104−3106.
(15) Akaike, T.; Ida, T.; Wei, F.-Y.; Nishida, M.; Kumagai, Y.; Alam, M. M.; Ihara, H.; Sawa, T.; Matsunaga, T.; Kasamatsu, S.; Nishimura, A.; Morita, M.; Tomizawa, K.; Nishimura, A.; Watanabe, S.; Inaba, K.; Shima, H.; Tanuma, N.; Jung, M.; Fujii, S.; Watanabe, Y.; Ohmuraya, M.; Nagy, P.; Feelisch, M.; Fukuto, J. M.; Motohashi, H. Cysteinyl-tRNA synthetase governs cysteine polysulfidation and mitochondrial bioenergetics. *Nat. Commun.* **2017**, *8*, 1177.
(16) Cuevasanta, E.; Lange, M.; Bonanata, J.; Coitiño, E. L.; Ferrer-Sueta, G.; Filipovic, M. R.; Alvarez, B. Reaction of Hydrogen Sulfide with Disulfide and Sulfenic Acid to Form the Strongly Nucleophilic Persulfide. *J. Biol. Chem.* **2015**, *290*, 26866−26880.
(17) Cuevasanta, E.; Reyes, A. M.; Zeida, A.; Mastrogiovanni, M.; De Armas, M. I.; Radi, R.; Alvarez, B.; Trujillo, M. Kinetics of formation and reactivity of the persulfide in the one-cysteine peroxiredoxin from Mycobacterium tuberculosis. *J. Biol. Chem.* **2019**, *294*, 13593−13605.
(18) Saund, S. S.; Sosa, V.; Henriquez, S.; Nguyen, Q. N. N.; Bianco, C. L.; Soeda, S.; Millikin, R.; White, C.; Le, H.; Ono, K.; Tantillo, D. J.; Kumagai, Y.; Akaike, T.; Lin, J.; Fukuto, J. M. The chemical biology of hydropersulfides (RSSH): Chemical stability, reactivity and redox roles. *Arch. Biochem. Biophys.* **2015**, *588*, 15−24.
(19) Millikin, R.; Bianco, C. L.; White, C.; Saund, S. S.; Henriquez, S.; Sosa, V.; Akaike, T.; Kumagai, Y.; Soeda, S.; Toscano, J. P.; Lin, J.; Fukuto, J. M. The chemical biology of protein hydropersulfides: Studies of a possible protective function of biological hydropersulfide generation. *Free Radical Biol. Med.* **2016**, *97*, 136−147.
(20) Shibata, A.; Ishima, Y.; Ikeda, M.; Sato, H.; Imafuku, T.; Chuang, V. T. G.; Ouchi, Y.; Abe, T.; Watanabe, H.; Ishida, T.; Otagiri, M.; Maruyama, T. Human serum albumin hydropersulfide is a potent reactive oxygen species scavenger in oxidative stress conditions such as chronic kidney disease. *Biochem. Biophys. Res. Commun.* **2016**, *479*, 578−583.
(21) Álvarez, L.; Bianco, C. L.; Toscano, J. P.; Lin, J.; Akaike, T.; Fukuto, J. M. Chemical Biology of Hydropersulfides and Related Species: Possible Roles in Cellular Protection and Redox Signaling. *Antioxid. Redox Signaling* **2017**, *27*, 622−633.
(22) Yang, C.-t.; Devarie-Baez, N. O.; Hamsath, A.; Fu, X.-d.; Xian, M. S-Persulfidation: Chemistry, Chemical Biology, and Significance in Health and Disease. *Antioxid. Redox Signaling* **2019**, DOI: 10.1089/ars.2019.7889.
(23) Bianco, C. L.; Chavez, T. A.; Sosa, V.; Saund, S. S.; Nguyen, Q. N. N.; Tantillo, D. J.; Ichimura, A. S.; Toscano, J. P.; Fukuto, J. M. The chemical biology of the persulfide (RSSH)/perthiyl (RSS·) redox couple and possible role in biological redox signaling. *Free Radical Biol. Med.* **2016**, *101*, 20−31.
(24) Chauvin, J.-P. R.; Griesser, M.; Pratt, D. A. Hydropersulfides: H-Atom Transfer Agents Par Excellence. *J. Am. Chem. Soc.* **2017**, *139*, 6484−6493.
(25) Fukuto, J. M.; Ignarro, L. J.; Nagy, P.; Wink, D. A.; Kevil, C. G.; Feelisch, M.; Cortese-Krott, M. M.; Bianco, C. L.; Kumagai, Y.; Hobbs, A. J.; Lin, J.; Ida, T.; Akaike, T. Biological hydropersulfides and related polysulfides − a new concept and perspective in redox biology. *FEBS Lett.* **2018**, *592*, 2140−2152.
(26) Bianco, C. L.; Akaike, T.; Ida, T.; Nagy, P.; Bogdandi, V.; Toscano, J. P.; Kumagai, Y.; Henderson, C. F.; Goddu, R. N.; Lin, J.; Fukuto, J. M. The reaction of hydrogen sulfide with disulfides: formation of a stable trisulfide and implications for biological systems. *Br. J. Pharmacol.* **2019**, *176*, 671−683.

(27) Lin, J.; Akiyama, M.; Bica, I.; Long, F. T.; Henderson, C. F.; Goddu, R. N.; Suarez, V.; Baker, B.; Ida, T.; Shinkai, Y.; Nagy, P.; Akaike, T.; Fukuto, J. M.; Kumagai, Y. The Uptake and Release of Polysulfur Cysteine Species by Cells: Physiological and Toxicological Implications. *Chem. Res. Toxicol.* **2019**, *32*, 447−455.
(28) Shinkai, Y.; Kumagai, Y. Sulfane Sulfur in Toxicology: A Novel Defense System Against Electrophilic Stress. *Toxicol. Sci.* **2019**, *170*, 3−9.
(29) Artaud, I.; Galardon, E. A Persulfide Analogue of the Nitrosothiol SNAP: Formation, Characterization and Reactivity. *ChemBioChem* **2014**, *15*, 2361−2364.
(30) Khodade, V. S.; Toscano, J. P. Development of S-Substituted Thioisothioureas as Efficient Hydropersulfide Precursors. *J. Am. Chem. Soc.* **2018**, *140*, 17333−17337.
(31) Zheng, Y.; Yu, B.; Li, Z.; Yuan, Z.; Organ, C. L.; Trivedi, R. K.; Wang, S.; Lefer, D. J.; Wang, B. An Esterase-Sensitive Prodrug Approach for Controllable Delivery of Persulfide Species. *Angew. Chem., Int. Ed.* **2017**, *56*, 11749−11753.
(32) Kang, J.; Xu, S.; Radford, M. N.; Zhang, W.; Kelly, S. S.; Day, J. J.; Xian, M. O→S Relay Deprotection: A General Approach to Controllable Donors of Reactive Sulfur Species. *Angew. Chem.* **2018**, *130*, 5995−5999.
(33) Powell, C. R.; Dillon, K. M.; Wang, Y.; Carrazzone, R. J.; Matson, J. B. A Persulfide Donor Responsive to Reactive Oxygen Species: Insights into Reactivity and Therapeutic Potential. *Angew. Chem., Int. Ed.* **2018**, *57*, 6324−6328.
(34) Bora, P.; Chauhan, P.; Manna, S.; Chakrapani, H. A Vinyl-Boronate Ester-Based Persulfide Donor Controllable by Hydrogen Peroxide, a Reactive Oxygen Species (ROS). *Org. Lett.* **2018**, *20*, 7916−7920.
(35) Saari, W. S.; Schwering, J. E.; Lyle, P. A.; Smith, S. J.; Engelhardt, E. L. Cyclization-activated prodrugs. Basic carbamates of 4-hydroxyanisole. *J. Med. Chem.* **1990**, *33*, 97−101.
(36) Gomes, P.; Vale, N.; Moreira, R. Cyclization-activated Prodrugs. *Molecules* **2007**, *12*, 2484−2506.
(37) Blencowe, C. A.; Russell, A. T.; Greco, F.; Hayes, W.; Thornthwaite, D. W. Self-immolative linkers in polymeric delivery systems. *Polym. Chem.* **2011**, *2*, 773−790.
(38) Zhao, Y.; Cerda, M. M.; Pluth, M. D. Fluorogenic hydrogen sulfide (H2S) donors based on sulfenyl thiocarbonates enable H2S tracking and quantification. *Chem. Sci.* **2019**, *10*, 1873−1878.
(39) Chengelis, C. P.; Neal, R. A. Studies of carbonyl sulfide toxicity: Metabolism by carbonic anhydrase. *Toxicol. Appl. Pharmacol.* **1980**, *55*, 198−202.
(40) Steiger, A. K.; Zhao, Y.; Pluth, M. D. Emerging Roles of Carbonyl Sulfide in Chemical Biology: Sulfide Transporter or Gasotransmitter? *Antioxid. Redox Signaling* **2018**, *28*, 1516−1532.
(41) Steiger, A. K.; Pardue, S.; Kevil, C. G.; Pluth, M. D. Self-Immolative Thiocarbamates Provide Access to Triggered H2S Donors and Analyte Replacement Fluorescent Probes. *J. Am. Chem. Soc.* **2016**, *138*, 7256−7259.
(42) Zhao, Y.; Pluth, M. D. Hydrogen Sulfide Donors Activated by Reactive Oxygen Species. *Angew. Chem., Int. Ed.* **2016**, *55*, 14638−14642.
(43) Powell, C. R.; Foster, J. C.; Okyere, B.; Theus, M. H.; Matson, J. B. Therapeutic Delivery of H2S via COS: Small Molecule and Polymeric Donors with Benign Byproducts. *J. Am. Chem. Soc.* **2016**, *138*, 13477−13480.
(44) Sharma, A. K.; Nair, M.; Chauhan, P.; Gupta, K.; Saini, D. K.; Chakrapani, H. Visible-Light-Triggered Uncaging of Carbonyl Sulfide for Hydrogen Sulfide (H2S) Release. *Org. Lett.* **2017**, *19*, 4822−4825.
(45) Powell, C. R.; Foster, J. C.; Swilley, S. N.; Kaur, K.; Scannelli, S. J.; Troya, D.; Matson, J. B. Self-amplified depolymerization of oligo(thiourethanes) for the release of COS/H2S. *Polym. Chem.* **2019**, *10*, 2991−2995.
(46) Zhao, Y.; Steiger, A. K.; Pluth, M. D. Cyclic Sulfenyl Thiocarbamates Release Carbonyl Sulfide and Hydrogen Sulfide Independently in Thiol-Promoted Pathways. *J. Am. Chem. Soc.* **2019**, *141*, 13610−13618.
(47) Chauhan, P.; Gupta, K.; Ravikumar, G.; Saini, D. K.; Chakrapani, H. Carbonyl Sulfide (COS) Donor Induced Protein Persulfidation Protects against Oxidative Stress. *Chem. - Asian J.* **2019**, *14*, 4717−4724.
(48) Hamid, H. A.; Tanaka, A.; Ida, T.; Nishimura, A.; Matsunaga, T.; Fujii, S.; Morita, M.; Sawa, T.; Fukuto, J. M.; Nagy, P.; Tsutsumi, R.; Motohashi, H.; Ihara, H.; Akaike, T. Polysulfide stabilization by tyrosine and hydroxyphenyl-containing derivatives that is important for a reactive sulfur metabolomics analysis. *Redox Biol.* **2019**, *21*, 101096.
(49) Cline, M. R.; Tu, C.; Silverman, D. N.; Toscano, J. P. Detection of nitroxyl (HNO) by membrane inlet mass spectrometry. *Free Radical Biol. Med.* **2011**, *50*, 1274−1279.
(50) pK_a is calculated using Advanced Chemistry Development (ACD/Laboratories) Software V11.02.
(51) Wang, Y.; Chun, O. K.; Song, W. O. Plasma and Dietary Antioxidant Status as Cardiovascular Disease Risk Factors: A Review of Human Studies. *Nutrients* **2013**, *5*, 2969−3004.
(52) Bajic, V. P.; Van Neste, C.; Obradovic, M.; Zafirovic, S.; Radak, D.; Bajic, V. B.; Essack, M.; Isenovic, E. R. Glutathione "Redox Homeostasis" and Its Relation to Cardiovascular Disease. *Oxid. Med. Cell. Longevity* **2019**, *2019*, 1.
(53) Effros, R. M.; Haider, B.; Ettinger, P. O.; Ahmed Sultan, S.; Oldewurtel, H. A.; Marold, K.; Regan, T. J. In vivo myocardial cell pH in the dog. Response to ischemia and infusion of alkali. *J. Clin. Invest.* **1975**, *55*, 1100−1110.
(54) Yan, G. X.; Kléber, A. G. Changes in extracellular and intracellular pH in ischemic rabbit papillary muscle. *Circ. Res.* **1992**, *71*, 460−470.
(55) Aldini, G.; Altomare, A.; Baron, G.; Vistoli, G.; Carini, M.; Borsani, L.; Sergio, F. N-Acetylcysteine as an antioxidant and disulphide breaking agent: the reasons why. *Free Radical Res.* **2018**, *52*, 751−762.
(56) Jones, L. J.; Singer, V. L. Fluorescence Microplate-Based Assay for Tumor Necrosis Factor Activity Using SYTOX Green Stain. *Anal. Biochem.* **2001**, *293*, 8−15.
(57) Ishiyama, M.; Miyazono, Y.; Sasamoto, K.; Ohkura, Y.; Ueno, K. A highly water-soluble disulfonated tetrazolium salt as a chromogenic indicator for NADH as well as cell viability. *Talanta* **1997**, *44*, 1299−1305.
(58) Tominaga, H.; Ishiyama, M.; Ohseto, F.; Sasamoto, K.; Hamamoto, T.; Suzuki, K.; Watanabe, M. A water-soluble tetrazolium salt useful for colorimetric cell viability assay. *Anal. Commun.* **1999**, *36*, 47−50.
(59) Pagliaro, P.; Mancardi, D.; Rastaldo, R.; Penna, C.; Gattullo, D.; Miranda, K. M.; Feelisch, M.; Wink, D. A.; Kass, D. A.; Paolocci, N. Nitroxyl affords thiol-sensitive myocardial protective effects akin to early preconditioning. *Free Radical Biol. Med.* **2003**, *34*, 33−43.
(60) Bell, R. M.; Mocanu, M. M.; Yellon, D. M. Retrograde heart perfusion: The Langendorff technique of isolated heart perfusion. *J. Mol. Cell. Cardiol.* **2011**, *50*, 940−950.
(61) Rossello, X.; Hall, A. R.; Bell, R. M.; Yellon, D. M. Characterization of the Langendorff Perfused Isolated Mouse Heart Model of Global Ischemia−Reperfusion Injury:Impact of Ischemia and Reperfusion Length on Infarct Size and LDH Release. *J. Cardiovasc. Pharmacol. Ther.* **2016**, *21*, 286−295.

https://dx.doi.org/10.1021/jacs.9b12180
J. Am. Chem. Soc. 2020, 142, 4309−4316